

## POT-CSA/ZnO Nanocomposites: Synthesis and Characterization

Alaa S. AL-Kabbi<sup>\*,†</sup>, Kahtan A. Mohammed<sup>†,§</sup> and  
Kareema M. Ziadan\*

\**Department of Physics, College of Science,  
Basrah University, Basrah, Iraq*

†*Department of Medical Physics,  
Hilla University College, Babylon, Iraq*

<sup>‡</sup>[fassth1960@gmail.com](mailto:fassth1960@gmail.com)

<sup>§</sup>[kahtan444@gmail.com](mailto:kahtan444@gmail.com)

Received 12 October 2022

Accepted 9 December 2022

Published 28 January 2023

To create a (POT-CSA/ZnO) nanocomposite, a chemical oxidative polymerization of O-toluidine was carried out in the presence of nano ZnO. This step took place throughout the synthesis. In the attendance of hydro chloric acid (HCl) and ammonium persulfate (APS) as an oxidant and camphor sulfonic acid (CSA) as a dopant, polymerization can be accomplished by using a monomer mixture with an equal molar ratio. Scanning electron microscope (SEM), X-ray diffraction (XRD), Fourier transform-infrared spectroscopy (FTIR), and UV–Vis spectroscopy were utilized in the procedure of characterizing the material. The results displayed that the polymer film revealed both excitonic transition  $\pi-\pi$  and to  $\pi-\pi^*$  transition. The semiconducting character of the composite can be confirmed by its electrical conductivity.

**Keywords:** Conducting polymer; ZnO; nanocomposites; optical properties; electrical properties.

### 1. Introduction

The easiness with which conducting polymer can be synthesized is a significant advantage. Conducting polymers can have their chemical structure modified in order to alter their chemical and physical properties such as their band gaps. They have a broad spectrum of electric conductivity, ranging from insulators value ( $10^{-9}$  S/cm) to metallic conductivity ( $10^5$ ) S/cm. In addition to being simple to produce and inexpensive, it is well known that these chemicals have low potential for poisoning.<sup>1</sup> Polyaniline (PANI) is a talented applicant for applied applications among polymers due to its respectable

environmental stability, easiness of production, high-temperature resistance, and the ability to tune its electrical conductivity from that of a conductor to that of an insulator by varying the type and concentration of dopant.<sup>2</sup> PANI has a number of drawbacks, the most significant of which is that it is infusible and cannot be dissolved in typical organic solvents. PANI and its synthetic derivatives have had their solvability and processability improved using a variety of alternative methodologies that have been designed. Unsubstituted PANI was shown to have a lower solubility compared to ring-substituted (alkyl and alkoxy) and N-alkyl-substituted PANI.<sup>3</sup>

Poly (o-toluidine) (o-toluidine) POT is derived from polyaniline, it has a methyl groups in the orthoposition of the aniline monomers. POT is perhaps the ring-substituted PANI derivative that has received the maximum attention and research throughout the years<sup>4</sup> because it is one of the promising polymers since it has been utilized in a variety of applications including solar cells, light-emitting diodes, field-effect transistors, schottky diodes, and sensors.<sup>5</sup>

There has been a rise in interest in conductive polymer-inorganic nanocomposites with a variety of component combinations in recent years. This is due to the fact that these materials exhibit intriguing physical features and have numerous possible applications in many different fields.<sup>6</sup> It was possible to synthesize nanocomposite by manipulating the compositions, structures, and morphologies of the component molecules.<sup>7</sup> During the polymerization process, the negatively charged inorganic nanoparticles are attracted to cationic monomers to form nanocomposite materials.<sup>7</sup> The manufacturing of many different devices has been made possible as a result of the ease with which organic polymers may be processed, in conjunction with the enhanced mechanical and optical capabilities of nanoparticles.<sup>8</sup> The improvements in the properties of these materials are brought about by the interactions between the polymer and the nanoparticles, in addition to the effects of state of dispersion.<sup>9</sup>

The preparation of nanocomposites consisting of POT and inorganic nanoparticles is an alternative road to enhance the properties of POT as well as the performances of nanofillers. The goal of this approach is to obtain materials with behaviors that are synergistic or balancing between POT and the nanoparticles.

ZnO nanoparticles have garnered a lot of attention among inorganic nanoparticles due to their one-of-a-kind catalytic, electrical, electronic, and optical capabilities, as well as their low cost and widespread applicability in a wide variety of fields.<sup>10</sup>

At ambient temperature, ZnO has a direct band gap of 3.3 eV and a significant exciton binding energy of 60 meV, making it a typical n-type semiconducting material found in nature. Its distinctive features also include a relatively wide direct band gap<sup>11</sup> in addition to being an essential electronic and photonic material with a wide variety of possible applications including light emitting diodes,

solar cells, transducers, photodetectors, and so on.<sup>6,12,13</sup>

Zinc oxide is a potential candidate due to its unique chemical, surface, and nanostructural properties; this makes it particularly useful for catalysis and gas sensing applications, both of which place a significant emphasis on the amount of particle surface area that is exposed to the gas of interest.<sup>14</sup>

The aim of this research work is to synthesize, characterize and study the structural, optical and morphological properties of POT-CSA/ZnO nanocomposite.

## 2. Experimental

### 2.1. Synthesis of POT-CSA/ZnO nanocomposite

The reaction was carried out in a three-necked flask fitted with a thermometer and stir bar, with 5 g of (O-toluidine) monomer dissolved in 100 ml of 1 M HCl with 0.05 g of ZnO nanoparticles and cooled to (Co), 22 ml of 1 M of camphor sulfonic acid (CSA), which is protonic acid was used as a dopant, and 15 g. After that, the contents of the reactor were stirred continuously for a full day. After being filtered to remove impurities, the dark green polymer precipitate was washed thrice in distilled water, thrice in acetone, twice in methanol, and then dried in an oven for 24 h to remove any moisture. At room temperature, powdered (POT-CSA/ZnO) was added to a solvent containing chloroform, and the mixture was stirred continuously.

### 2.2. Thin film preparation

When making the POT solution, chloroform was used as the solvent. After being thoroughly mixed, the solution was dropped by the drop onto 2 × 2 cm glass substrates, which were then spun at 1000 rpm for 30 s.

## 3. Results and Discussion

XRD procedure was used to characterize the structures of the chemically synthesized POT-CSA/ZnO films. The XRD pattern of the POT-CSA/ZnO nanocomposite, as illustrated in Fig. 1, was recorded in 2θ range of the order of 10–60°. X ray diffraction pattern showed that the POT-CSA/ZnO

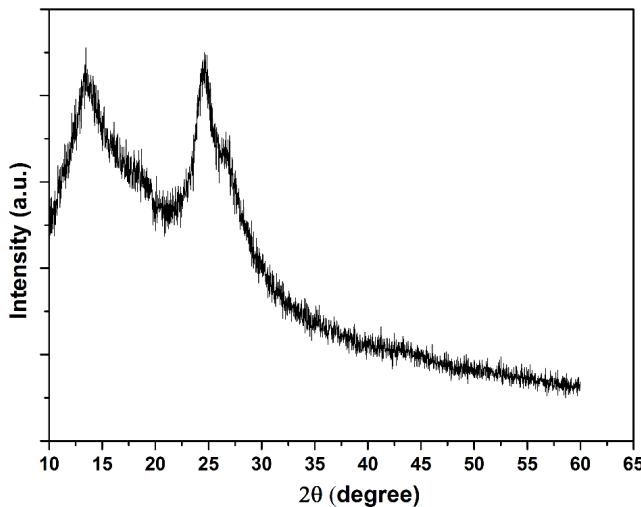


Fig. 1. XRD patterns of POT–ZnO composite.

has semi-crystalline nature with two broad diffraction peaks with the first one at  $2\theta = 13.5^\circ$ . A crystalline peak appearing at  $14.9^\circ$  has been reported with PANI,<sup>15</sup> also copolymer doped with CSA indicates the crystalline camphor sulfonic acid.<sup>16</sup> Similarly, a new peak was observed in PPy–ZnO–CSA thin film.<sup>17</sup> The second one at  $2\theta = 23.6^\circ$ . In other words, the interaction of polymer and ZnO nanoparticles led to an increase in the crystallinity of the polymer. The presence of ZnO in the polymerization system has a significant impact on the crystalline behavior of the produced polymer.

Figure 2 presents an illustration of the FTIR spectrum of the POT–CSA/ZnO nanocomposites. The ZnO stretching mode is connected to the bands located at 494, which belong to ZnO. The C–H stretching vibration of the methyl group is responsible for the peak that is observed at  $2847\text{ cm}^{-1}$ .<sup>16</sup> Peak at  $2353\text{ cm}^{-1}$  could be due to NH<sup>+</sup> stretching of the amine group, according to Refs. 18 and 19. According to what was seen in the spectra, the quinoid band has a peak at  $1583\text{ cm}^{-1}$ , while the benzenoid band has a peak at  $1482\text{ cm}^{-1}$ . This suggests that the nature of the composite is that it contains emeraldine salt, which indicates that it is a conductive form of POT.<sup>20,21</sup> Research found that the band with a frequency range of  $1100\text{--}1160\text{ cm}^{-1}$  was associated with an aromatic C–N stretching vibration of  $1020\text{ cm}^{-1}$  because the CSA has a group called SO<sub>3</sub>, which is responsible for interactions between sulfur and oxygen.<sup>22</sup> A C–H out-of-plane bending vibration was assigned to the peak at 553.<sup>23</sup>

Figure 3 displays the FESEM image of the synthesized POT–CSA/ZnO nanocomposites. It shows that o-toluidine monomer was polymerized around ZnO particle to form POT–CSA/ZnO nanocomposite. The particles are disorderly spherical clusters with the size of about 100 nm.

The ultraviolet to visible spectrum of the POT/ZnO thin films was investigated in great detail. Recordings of spectra of absorption were made. The absorption spectra of POT–ZnO may be shown in

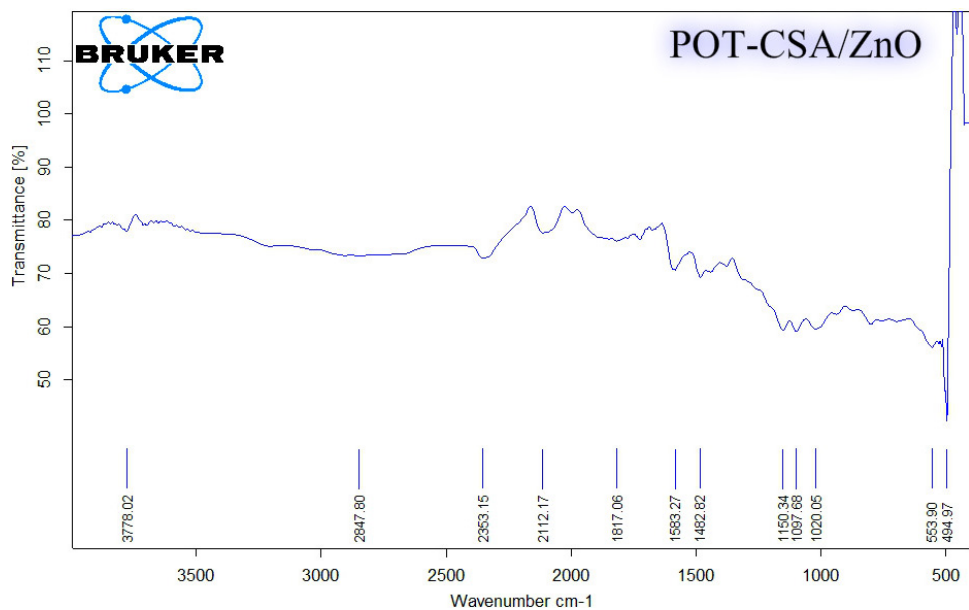


Fig. 2. FTIR spectrum of POT–ZnO composite.

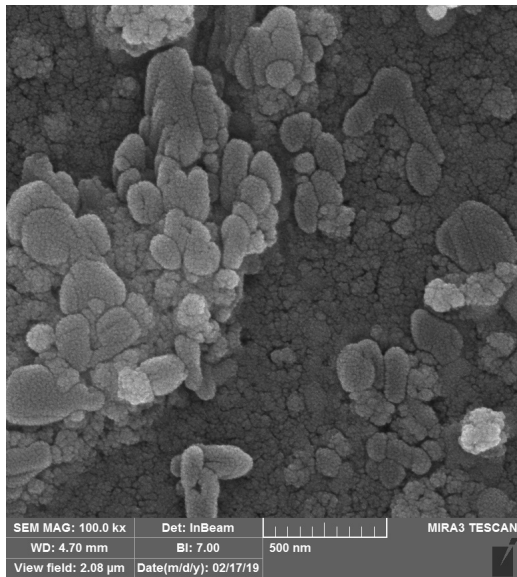


Fig. 3. FESEM image of POT–ZnO composite.

Fig. 4, along with its absorption coefficient. The development of doped POT can be verified by the presence of three distinctive absorption bands at around 310, 415, and 830 nm.<sup>24</sup> The  $\pi-\pi^*$  exciton transition may be responsible for the band that is located at around 325 nm.<sup>25</sup> The amount of doping in POT is responsible for the second shoulder-like absorption band that was observed at 415 nm.<sup>22</sup> Additionally, the conducting emeraldine salt phase is responsible for the third absorption peak that occurs about 820 nm.

Absorption coefficient ( $\alpha$ ) of the film is calculated using relation<sup>26</sup>

$$\alpha = (A * 2.303)/t. \quad (1)$$

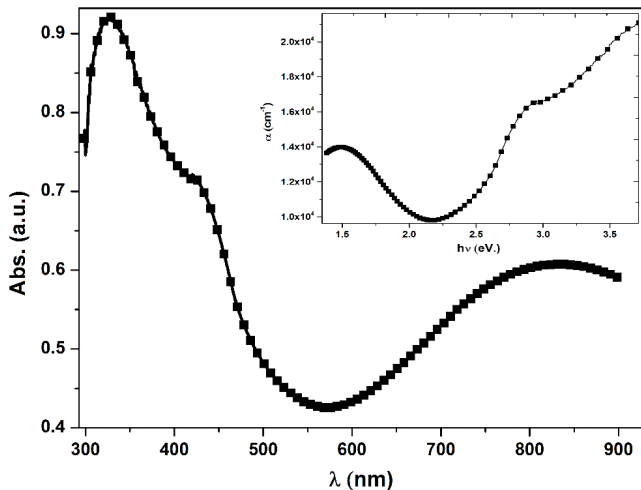


Fig. 4. Absorption spectrum of POT–ZnO composite.

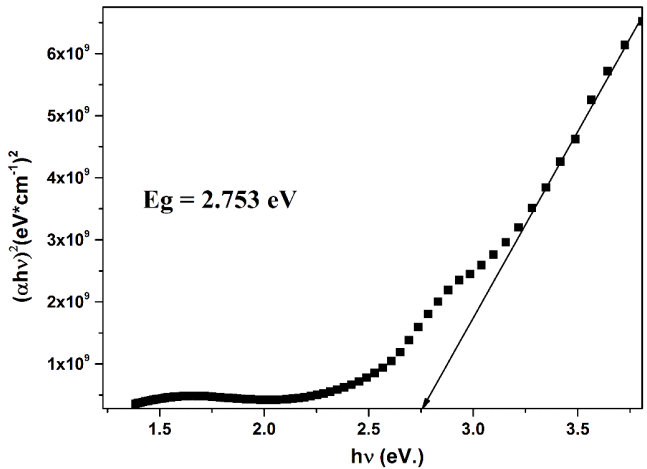


Fig. 5. Band gap of POT–ZnO composite.

The separation of the highest occupied molecular orbital and the lowest empty molecular orbital is reflected in the optical band gap. Tauc's formula for permitted direct transitions was used to calculate the optical band gap.<sup>27</sup>

Figure 5 shows the bandgap of POT–ZnO composite. The measured value of the optical band gap is 2.75.

The electrical properties of nanocomposite were tested. Figure 6 displays the alternation of current–voltage (I–V) characteristics of POT–CSA/ZnO nanocomposite tested at room temperature. We observe from the figure that the I–V curves are linear. The conductivity value is calculated from the current via the following equation:

$$\sigma = \frac{Is}{Vdl}, \quad (2)$$

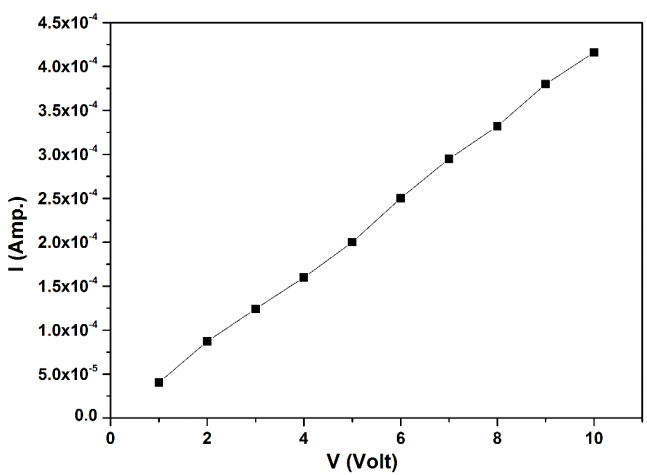


Fig. 6.  $I - V$  of POT–ZnO composite.

where  $s$  is the width between the electrodes,  $V$  is the applied voltage between the electrodes,  $d$  is the sample thickness and  $l$  is the length of electrodes.

The dark conductivity of the nanocomposite film at room temperature was equal  $4 \times 10^{-2}$  S/cm<sup>2</sup>.

#### 4. Conclusion

In this paper, the POT-CSA/ZnO nanocomposite was chemically synthesized by *in-situ* polymerization. The XRD patterns showed that the composite combined the diffraction peak from ZnO and the peak from the POT. FT-IR spectra indicated that there was an interaction between POT and ZnO in the composite. Good electrical and optical properties have been accomplished and the nanocomposite is suitable for optoelectronic applications.

#### References

1. K. M. Z. D. KThabyh, *Adv. Phys. Theor. Appl.* **42**, 1 (2016).
2. K. Sivakumar, V. Senthil Kumar and Y. Haldorai, *Compos. Interfaces* **19**, 397 (2012).
3. T. Abdiryim, Z. Xiao-Gang and R. Jamal, *J. Appl. Polym. Sci.* **96**, 1630 (2005).
4. K. A. Mohammed, K. M. Ziadan, A. S. Al-Kabbi, D. S. Abdulzahr, H. K. Judi and H. M. Hussein, The role of formic acid as secondary dopant and solvent for poly (o-toluidine) intrinsically doped with camphor sulfonic acid, in *Materials Science Forum*, Vol. 1039 (Trans Tech Publications Ltd., Switzerland, 2021), pp. 260–268.
5. R. F. Alfahed and K. I. Ajeel, *Int. J. Mater. Sci. Eng.* **3**, 319 (2015).
6. A. A. Khan and M. Khalid, *J. Appl. Polym. Sci.* **117**, 1601 (2010).
7. S. C. Tjong and Y. W. Mai (eds.), *Physical Properties and Applications of Polymer Nanocomposites* (Elsevier, Amsterdam, 2010).
8. Rajesh, T. Ahuja and D. Kumar, *Sens. Actuators B Chem.* **136**, 275 (2009).
9. S. Islam, S. Ahmad and H. Khan, *J. Mater. Sci. Mater. Electron.* **29**, 13241 (2018).
10. Y. He, *Appl. Surf. Sci.* **249**, 1 (2005).
11. M. L. Singla, R. Sehrawat, N. Rana and K. Singh, *J. Nanoparticle Res.* **13**, 2109 (2011).
12. B. K. Sharma, A. K. Gupta, N. Khare, S. K. Dhawan and H. C. Gupta, *Synth. Met.* **159**, 391 (2009).
13. M. A. Haque and S. Mahalakshmi, *Res. Chem. Intermed.* **41**, 5205 (2015).
14. A. Ghosh *et al.*, *J. Alloys Compd.* **469**, 56 (2009).
15. W. Y. Zou, W. Wang, B. L. He, M. L. Sun and Y. S. Yin, *J. Power Sources* **195**, 7489 (2010).
16. A. Mahudeswaran, D. Manoharan, J. Chandrasekaran, J. Vivekanandan and P. S. Vijayanand, *Mater. Res.* **18**, 482 (2015).
17. M. A. Chougule, G. D. Khuspe, S. Sen and V. B. Patil, *Appl. Nanosci.* **3**, 423 (2013).
18. V. D. Deepak Verma, *Sens. Actuators B* **134**, 373 (2008).
19. A. A. M. Farag, A. Ashery and M. A. Shenashen, *Physica B Condens. Matter* **407**, 2404 (2012).
20. H. K. Patil, M. A. Deshmukh, G. A. Bodkhe and S. M. Shirsat, *Appl. Phys. A* **124**, 1 (2018).
21. V. V. Chabukswar *et al.*, *J. Macromol. Sci. A* **51**, 435 (2014).
22. M. V. Kulkarni, A. K. Viswanath and P. K. Khanna, *J. Polym. Eng.* **26**, 487 (2006).
23. M. V. Kulkarni and A. K. Viswanath, *Eur. Polym. J.* **40**, 379 (2004).
24. K. A. Mohammed, K. M. Ziadan, A. S. Al-Kabbi, R. S. Zabibah and A. J. Alrubaie, *Int. J. Nanosci.* **20**, 2150059 (2021).
25. A. Kumar, V. Ali and S. Kumar, *J. Macromol. Sci. B* **52**, 1107 (2013).
26. P. K. Sahu, R. Das and R. Lalwani, *Appl. Phys. A Mater. Sci. Process.* **124**, 487 (2018).
27. N. M. Hosny, G. Samir, M. S. Zoromba and S. Alghool, *Polym. Plast. Technol. Eng.* **56**, 435 (2017).